Meckelin Is Necessary for Photoreceptor Intraciliary Transport and Outer Segment Morphogenesis

Gayle B. Collin, Jungyeon Won, Wanda L. Hicks, Susan A. Cook, Patsy M. Nishina, and Jürgen K. Naggert

Purpose. Cilia, complex structures found ubiquitously in most vertebrate cells, serve a variety of functions ranging from cell and fluid movement, cell signaling, tissue homeostasis, to sensory perception. Meckelin is a component of ciliary and cell membranes and is encoded by *Tmem67* (*Mks3*). In this study, the retinal morphology and ciliary function in a mouse model for Meckel Syndrome Type 3 (MKS3) throughout the course of photoreceptor development was examined.

Methods. To study the effects of a disruption in the *Mks3* gene on the retina, the authors introduced a functional allele of *Pde6b* into *B6C3Fe a/a-bpck/J* mice and evaluated their retinas by ophthalmoscopic, histologic, and ultrastructural examination. In addition, immunofluorescence microscopy was used to assess protein trafficking through the connecting cilium and to examine the localization of ciliary and synaptic proteins in *Tmem67*^{bpck} mice and controls.

Results. Photoreceptors degenerate early and rapidly in *bpck/bpck* mutant mice. In addition, phototransduction proteins, such as rhodopsin, arrestin, and transducin, are mislocalized. Ultrastructural examination of photoreceptors reveal morphologically intact connecting cilia but dysmorphic and misoriented outer segment (OS) discs, at the earliest time point examined.

Conclusions. These findings underscore the important role for meckelin in intraciliary transport of phototransduction molecules and their effects on subsequent OS morphogenesis and maintenance. (*Invest Ophthalmol Vis Sci.* 2012;53:967–974) DOI:10.1167/iovs.11-8766

Meckelin is a transmembrane ciliary protein encoded by the *MKS3/TMEM67* gene.[1] Patients with mutations in *MKS3/TMEM67* develop phenotypically similar disorders including Meckel–Gruber Syndrome Type 3,[1] Bardet–Biedl Syndrome,[2] COACH (cerebellar vermis hypoplasia/aplasia, oligophrenia, ataxia, coloboma, and hepatic fibrosis) syndrome,[3,4] Joubert Syndrome,[5] and Nephronophthisis (NPHP11).[6] Meckel–Gruber Syndrome, first described by Meckel in 1822, is a recessively inherited perinatal lethal condition characterized by central nervous system (CNS) abnormalities including occipital encephalocele, bilateral polycystic kidney disease (PKD), biliary dysgenesis, and polydactyly.[7] Joubert and COACH syndromes result in cerebellar vermis hypoplasia and hypotonia, developmental delay, neonatal respiratory defects, and oculomotor apraxia. Patients with Joubert Syndrome, type B are characterized by retinal and renal impairment.[5]

In Meckel–Gruber Syndrome (MKS), locus heterogeneity exists, in that disruptions in seven other genes—*MKS1*, *TMEM216*, *RPGRIP1L*, *CEP290*, *CC2D29*, *B9D1*, and *TCTN2*—also result in the typical clinical features observed in MKS.[1,8–13] The proteins encoded by these genes are found at the transition zone in ciliated cells.[14,15] However, some of these proteins also localize to other regions, that is, MKS1 and TMEM216 in the basal bodies and MKS3 at the plasma and ciliary membranes.[14,16]

Many mutations in genes that encode proteins localizing to the connecting cilium (CC) and/or its basal body—*NPHP4*, *RP1*, *RPGRIP1*, *NPHP6* (*CEP290*), *BBS4*, *AHI1*—lead to ciliary dysfunction in the retina and result in the mislocalization of outer segment (OS) proteins and disorganization of the OSs.[17–23] Some of these proteins have roles in intraflagellar transport (IFT). In retinal photoreceptors, IFT involves a process by which motor-driven subcomplexes move proteins from the inner segments (ISs) along the axoneme of the CC, a modified sensory cilium, to the OS. Therefore, IFT is essential for the assembly and maintenance of OS discs.[24,25]

In mammalian photoreceptors, OS disc shedding and restoration occur continuously, with a turnover rate of 10% per day.[26] Thus, the trafficking of disc proteins is crucial not only for OS assembly, but also for their maintenance throughout the life of the cell.[27] Disruption of any of the processes necessary for intracellular transport through the CC is likely to impair proper cell function. At the microtubule-organizing center, loading of cargo onto the microtubules can also be affected or the axonemal network itself may be structurally or functionally compromised. Additionally, aberrant polarity and orientation of photoreceptors may affect OS disc stacking and shedding.[18] Defects in any of these processes that involve the CC[28] may contribute to the OS loss that precedes photoreceptor degeneration.

Recently, we described a mouse model for Meckel Syndrome Type 3 (MKS3), B6C3Fe *a/a-bpck/J*, with clinical features similar to those reported for patients with Meckel–Gruber Syndrome.[29] *Tmem67*^{bpck} (*bpck/bpck*) mutant mice, which carry a 295-kilobase deletion encompassing six genes, develop bilateral polycystic kidney disease, hydrocephaly, and premature death. In this study, we characterized the retinas of *Tmem67*^{bpck} mice throughout the course of photoreceptor development and identified deficits in intraciliary transport and outer segment morphogenesis.

Methods

Mouse Husbandry

B6C3Fe *a/a-bpck/J* and *Tmem67*-expressing transgenic mice[29] were bred and maintained in the Research Animal Facility at The Jackson

From The Jackson Laboratory, Bar Harbor, Maine.

Supported in part by National Institutes of Health (NIH)/National Institute of Child Health and Human Development Grant HD036878 (JKN, GBC), NIH/National Eye Institute Grant EY016501 (PMN, WLH, JW), and NIH/National Cancer Institute Grant CA34196.

Submitted for publication October 7, 2011; revised December 21, 2011; accepted December 30, 2011.

Disclosure: **G.B. Collin**, None; **J. Won**, None; **W.L. Hicks**, None; **S.A. Cook**, None; **P.M. Nishina**, None; **J.K. Naggert**, None

Corresponding author: Jürgen K. Naggert, The Jackson Laboratory, 600 Main Street, Bar Harbor, ME 04609; juergen.naggert@jax.org.

Laboratory (JAX). Mice were fed a normal chow diet (5K54 LabDiet JAX Mice, 4% fat; Laboratory Diets) and acidified water without restriction and were maintained in a 12:12-hour dark-to-light cycle. All mouse procedures used in this study were approved by the JAX institutional Animal Care and Use Committee. Since B6C3Fe *a/a-bpck/J* was homozygous for the *Pde6b*^{rd1} mutation (common to C3H backgrounds), effects of the loss of MKS3 function on the retina could not be assessed. Therefore, we outcrossed them to C57BL/6J mice to introduce a functional *Pde6b* allele (wild-type at the *rd1* locus), with double heterozygotes (*bpck/*+, *rd1/*+) for the subsequent intercross generations. *bpck/bpck*, *Pde6b*$^{rd1+/+}$ mice were used for the studies described herein.

DNA Extraction and Genotyping

Genomic DNA was isolated from tail tips by proteinase K digestion and salt precipitation.[30] PCR conditions for genotyping the *bpck* mutation were as follows: genomic DNA was denatured at 94°C for 2 minutes, followed by 45 cycles of 94°C for 30 seconds, 54°C for 30 seconds, 72°C for 40 seconds, and a final extension of 72°C for 7 minutes.

Primers used to identify mice carrying the mutated allele were: *Cdh17F10*, CCCTTTTGTCAAGAAAGATG and *C430048L16RikF*, GCAGTCTGCCTCTCACTAAC. Primers used to detect the wild-type allele were: *Tmem67F12*, GAAGAGCAGCACCGTTACCT and *Tmem67R12*, GCCACTTGCTGGAGCTACTGT.

PCR conditions for genotyping for the *Pde6b*^{rd1} mutation was as follows: genomic DNA was denatured at 94°C for 5 minutes, followed by 35 cycles of 94°C for 30 seconds, 65°C for 30 seconds, 72°C for 90 seconds, and a final extension of 72°C for 2 minutes. Primers used: F1, AAGCTAGCTGCAGTAACGCCATTT; F2, ACCTGCATGTGAACCCAGTATTCTATC; and R1, CTACAGCCCCCTCTCCAAGGTTTATAG. F1/R1 amplifies a 560–base pair (bp) fragment (mutant allele) and F2/R1 amplifies a 240-bp fragment (wild-type allele).

PCR amplicons were separated on a 2% agarose gel and visualized with ethidium bromide under UV light illumination.

Ultrastructural Analysis

For TEM analysis, eyes were fixed in a 2.5% gluteraldehyde/2% paraformaldehyde (PFA) solution in phosphate buffer (Sørensen's Buffer; Sigma-Aldrich). Tissues were dissected as previously described,[20] postfixed in osmium tetroxide, dehydrated, and embedded in plastic. Sections were stained with uranyl acetate and lead citrate and examined using a transmission electron microscope (JEM-1230; JEOL, Tokyo, Japan).

For SEM analysis, retinas were dissected from the retinal pigment epithelium (RPE) and fixed in 3% gluteraldehyde and 1% PFA solution for 2 to 4 hours at 4°C. Tissues were postfixed in osmium tetroxide, dehydrated, dried with hexamethyldisilazane, and sputter coated. Specimens were mounted and examined by SEM at 20 kV (Hitachi Technologies America, Parsippany, NJ).

Antibodies

The following antibodies were used: anti-SYPH (1:200; Santa Cruz Biotechnology, Santa Cruz, CA); anti-ribeye (CTBP2, 1:300; BD Biosciences, Billerica, MA), anti-red/green opsin (1:200; Millipore [formerly Chemicon], Billerica, MA), anti-OPN1SW (blue opsin, 1:200; Santa Cruz Biotechnology), anti-rhodopsin (1:500; Leinco Technologies, Fenton, MO), anti-ROM1 (1:500; a kind gift from R. McInnes), anti-rod transducin (GNAT1, 1:200; Santa Cruz Biotechnology), anti-rod arrestin (1:500; ABR, Inc., Pullman, WA), anti-Alms1-Ntr (1:300; a kind gift from Tom Hearn), anti-NPHP4 (1:50[17]), anti-RP1 (1:500; a kind gift from Eric Pierce), anti-RPGRIP1L (1:250; a kind gift from Ronald Roepman), and anti-RPGR (1:300; a kind gift from Tiansen Li).

Histologic and Immunohistochemical Analysis

Mouse eyes were fixed overnight in cold methanol:acetic acid:phosphate buffer solution (3:1:4 v/v) or 4% PFA. Eyes were oriented by optic nerve position, paraffin-embedded, and sectioned. For histology, deparaffinated tissue sections were stained with hematoxylin and eosin and examined by light microscopy. For immunohistochemical analysis, deparaffinated and cryopreserved tissues were incubated with primary antibodies at 4°C overnight. The following day, fluorescently labeled secondary antibodies (Cy3, FITC; Alexa Fluor 488 or Alexa Fluor 549; Invitrogen) were incubated with tissue for 45 minutes at room temperature, washed in PBS, and visualized with an upright fluorescent microscope (Leica Microsystems, Wetzlar, Germany). For retinal whole mount, eyes were fixed in cold 4% PFA for 30 minutes. Cornea and lens were removed and retinas were cut radially to flatten the tissue. Whole mounts were blocked in 20% serum in phosphate-buffered saline Tween-20 (PBST solution, 0.2%) for 1 hour and labeled with blue cone opsin (1:200) or red/green opsin (1:200) for 12 to 18 hours at 4°C. Tissues were washed in PBS and incubated in Cy3-conjugated secondary and PNA-lectin in 10% serum in PBST for 3 hours. Fluorescent staining was visualized using a research-grade microscope (DMLB; Leica Microsystems) or a high-end materials microscopy platform (AxioObserver.Z1m; Carl Zeiss Meditec AG, Berlin, Germany) with ApoTome microscope (Carl Zeiss Meditec AG).

Results

Early Onset and Rapid Retinal Degeneration in *bpck/bpck* Mutants

Ophthalmic examination at 21 days revealed a granular fundus appearance (not shown). By 34 days, multiple dysmorphic

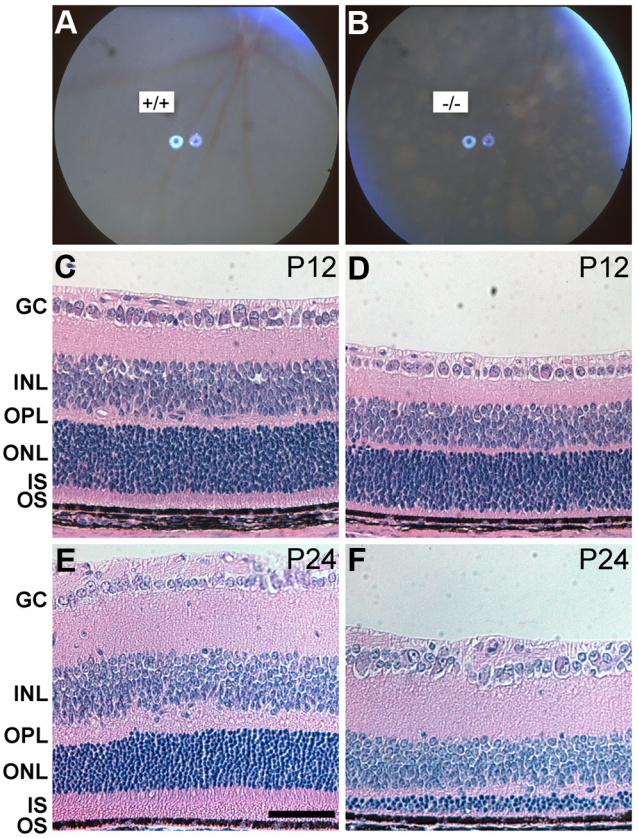

Figure 1. Retinal degeneration in the *Tmem67*^{bpck} mouse model. Fundus photographs at P34 of (**A**) wild-type (+/+) control retina and (**B**) *bpck/bpck* (−/−) mutant retina. H&E–stained retinas of controls (**C**, **E**) and mutants (**D**, **F**) at P12 and P24, respectively, show an early onset and progressive photoreceptor degeneration in *bpck/bpck* mutants. GC, ganglion cell; INL, inner nuclear layer; OPL, outer plexiform layer. Scale bar: 50 μm.

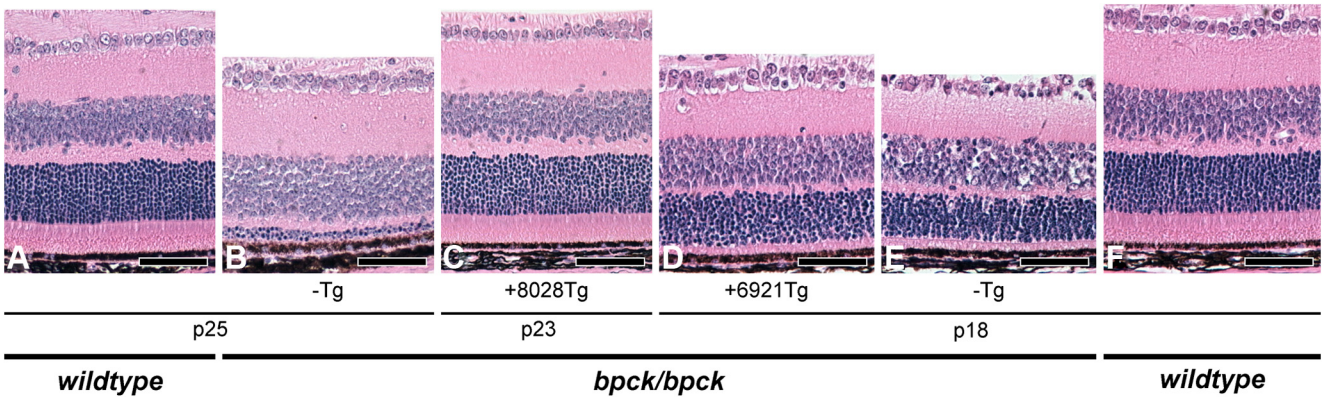

Figure 2. Micrographs demonstrating the effects of a BAC transgenic rescue in mutant mice overexpressing the *Mks3* gene. (**A**, **F**) Wild-type controls at P25 and P18, respectively. (**B**, **E**) *bpck/bpck* mutants without transgene show a lack of OS at P18 and a major loss of photoreceptor cells at P25. (**C**) A complete rescue of photoreceptor degeneration in P23 *bpck/bpck* mice crossed to the 8028 transgenic line overexpressing *Mks3*. (**D**) P18 *bpck/bpck* mice with a BAC transgene lacking *Mks3* (6921Tg) failed to rescue the retinal phenotype: photoreceptors lack OS. Note: 6921Tg mice overexpress *Ppm2c*, *1700123M08Rik*, and *Gm10604*; 8028Tg mice overexpress *Ppm2c*, *1700123M08Rik*, *Gm10604*, and *Tmem67*. Scale bar: 50 μm.

patches and attenuation of retinal blood vessels were observed in the fundus of homozygous mutants (Figs. 1A, 1B).

Histologically, *bpck/bpck* retinas show an early, rapid progressive loss of photoreceptors (Figs. 1C–F). By light microscopy, at P12, whereas no quantifiable differences in the ONL were observed between mutants and controls, inner segments were thinned and OSs were not clearly visible in mutants. By P24, the photoreceptor ONL was reduced to three to four rows of nuclei and the outer plexiform layer (OPL), the layer containing the peripheral region and secondary neuron synapses was markedly shortened in mutant retinas. Because six genes, including *Mks3*, *Cdh17*, *Ppm2c*, *Gm10604*, *C430048L16Rik*, and *1700123M08Rik*, are affected by the large deletion in *bpck/bpck* mice,[29] we sought to confirm that the deletion of *Mks3* was indeed the cause of the early retinal degeneration in these mutant mice. We examined retinas from previously described transgenic rescue lines with and without *Mks3*. Histochemical examination showed that the transgenic line overexpressing *Mks3* (8028Tg) rescued the retinal degeneration in the *bpck/bpck* mice, whereas the transgenic line without *Mks3* (6921Tg) failed to normalize the retinal phenotype (Fig. 2). The transgenic lines overexpressing *Mks3* rescued the polycystic kidney and hydrocephaly phenotypes as well, confirming that the deletion of *Mks3* is the cause of the syndromic disorder observed.

bpck/bpck Mice Have a Normal OPL Synaptic Architecture but Fail to Develop Proper OS Discs

Since light micrographs revealed that mutant retinas had OPLs that were significantly shorter than OPLs from control mice at 24 weeks of age, we examined the synapses in the OPL by immunostaining and by ultrastructural analysis. Staining with anti-SYPH showed similar synaptic staining between mutants

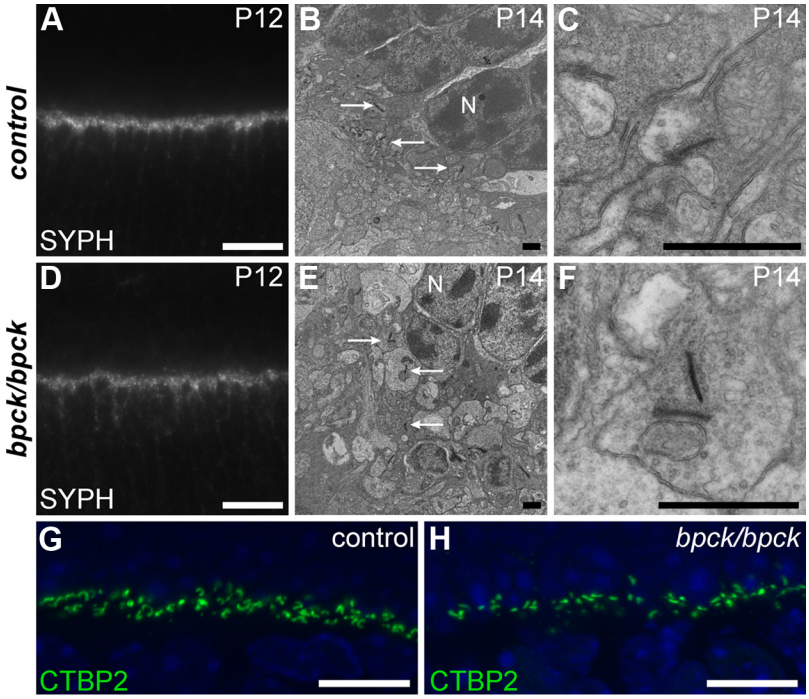

Figure 3. Examination of synapses in the OPL (**A**, **D**). Immunostaining with synaptophysin (SYPH) shows similar staining patterns between controls (**A**) and mutants (**D**). Transmission electron micrographs (TEMs) show normal synapses and synaptic vesicles at the synaptic junctions of the mutants (**E**, **F**) compared with controls (**B**, **C**). (**G**, **H**) Immunostaining with ribeye (CTBP2) shows fewer synaptic ribbons in mutants compared with controls at P14. Scale bars: (**A**, **D**) 20 μm; (**B**, **C**, **E**, **F**) 1 μm; (**G**, **H**) 10 μm.

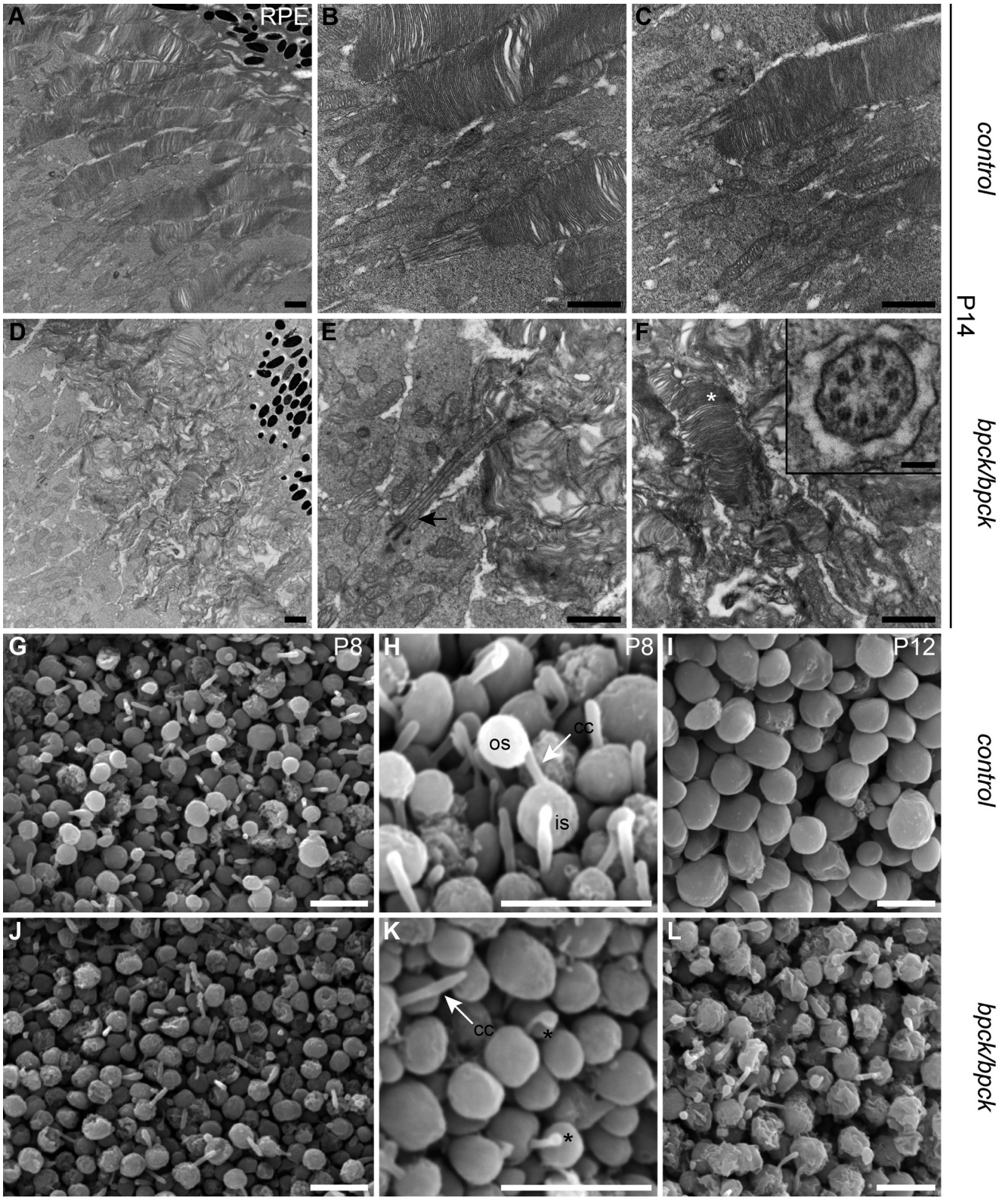

Figure 4. Ultrastructural imaging reveals normal ciliary architecture but disorganized outer segments. TEM image of (**A–C**) P14 normal retina. The CC and inner and outer segments display intact architecture with well-ordered stacks of membranous OS discs. (**D–F**) P14 *bpck/bpck* mutant retina. Microtubules of the ciliary axoneme appear structurally intact. (**F**) *Inset*: cross-section of the ciliary axoneme shows typical "9+0" microtubule arrangement. OS discs are amorphous and disorganized. Although a few stacks of membranous discs are observed, the majority are significantly shortened and disorganized. (**G–L**) Scanning electron images reveal a failure of proper OS development in *bpck/bpck* mutants in P8 and P12 photoreceptors. In controls (**G**, **H**), at P8, rudimentary OSs emerging from CCs are observed, whereas by P12 (**I**), OSs have elongated to form columnar structures. In contrast, in *bpck/bpck* photoreceptors, at P8 (**J**, **K**) rudimentary budding OSs (*asterisk*) are rarely observed. At P12 (**L**), the few OSs that are observed are clearly malformed. Scale bars: (**A–F**) 1 μm; (**G–L**) 5 μm; (**F**, *inset*) 100 nm.

and controls at P12 (Figs. 3A, 3D). Transmission electron microscopy (TEM) of P14 retinas revealed normal architecture of synapses and vesicles at the OPL synaptic junctions in both control and mutants (Figs. 3B, 3C, 3E, 3F). However, staining with anti-RIBEYE (CTBP2) showed visibly fewer synapses in *bpck/bpck* mice than that in controls at P14 (Figs. 3G, 3H).

OSs were not evident by light microscopy in 3-week-old *wpk/wpk* rats or *bpck/bpck* mice (Fig. 1).[31] To determine whether OSs are ever formed in *bpck/bpck* mutants, we examined photoreceptor ultrastructure by TEM analysis (Figs. 4A–F). OSs, which were rarely observed at P14 in mutant mice, appeared misshapened and disorganized. We also examined OS formation in mutant retinas by scanning electron microscopy during photoreceptor development (Figs. 4G–L). OSs failed to develop normally in mutant mice. By P12, when OSs of wild-type retinas appeared as uniform columnar structures, most CCs did not bear OSs and the OSs that were observed were dysmorphic in mutant retinas.

To determine whether *bpck/bpck* mice undergo normal ciliogenesis, photoreceptor cilia were also examined by transmission and scanning electron microscopy for ultrastructural defects. At P14, the structure of the CC and its basal body and inner segments appeared normal (Figs. 4A–F). Additionally, in cross-section, the ciliary axoneme of homozygous *Tmem67*^{bpck} mutants had a normal "9+0" arrangement of microtubules. Scanning micrographs of mutant photoreceptors at P8 show that CCs were clearly visible (Figs. 4G–L). By P12, although OSs were rarely observed in mutants compared with the controls, CCs projected from ISs.

Defects in Movement of Proteins through the Connecting Cilium

To determine whether meckelin has a role in intraciliary transport of proteins through the CC, we examined, by immunohistochemistry, the localization of several proteins known to be transported from the inner segments to the outer segments via the CCs (Fig. 5). Unlike models of slowly progressive retinal degeneration (i.e., Alström Syndrome), staining of rhodopsin and ROM1 was absent in the OS of *bpck/bpck* mice. As early as P12, both proteins mislocalized entirely to the inner segments and ONL (Figs. 5A–D). To determine whether there were abnormalities in the movement of OS proteins in mice lacking MKS3, the translocation of arrestin and transducin in P14 mutant and control pups was examined. In retinas obtained from dark-adapted *bpck/bpck* mice, transducin was aberrantly distributed in the inner segments and cell bodies in the ONL (Figs. 5G, 5P). When mutant retinas were exposed to light, signs of impaired translocation were evident because arrestin failed to move from the ONL and IS to the OS (Figs. 5K, 5L, 5T).

Localization of Ciliary Proteins in *bpck/bpck* Mice

We used fluorescent microscopy to examine the localization of photoreceptor ciliary proteins in *bpck/bpck* mutant and control mice. Immunostained images of RPGRIP1L (ciliary transition zone[15]), ALMS1 (basal bodies[32]), and RPGR (transition zone and CC[33]) showed normal localization of these proteins

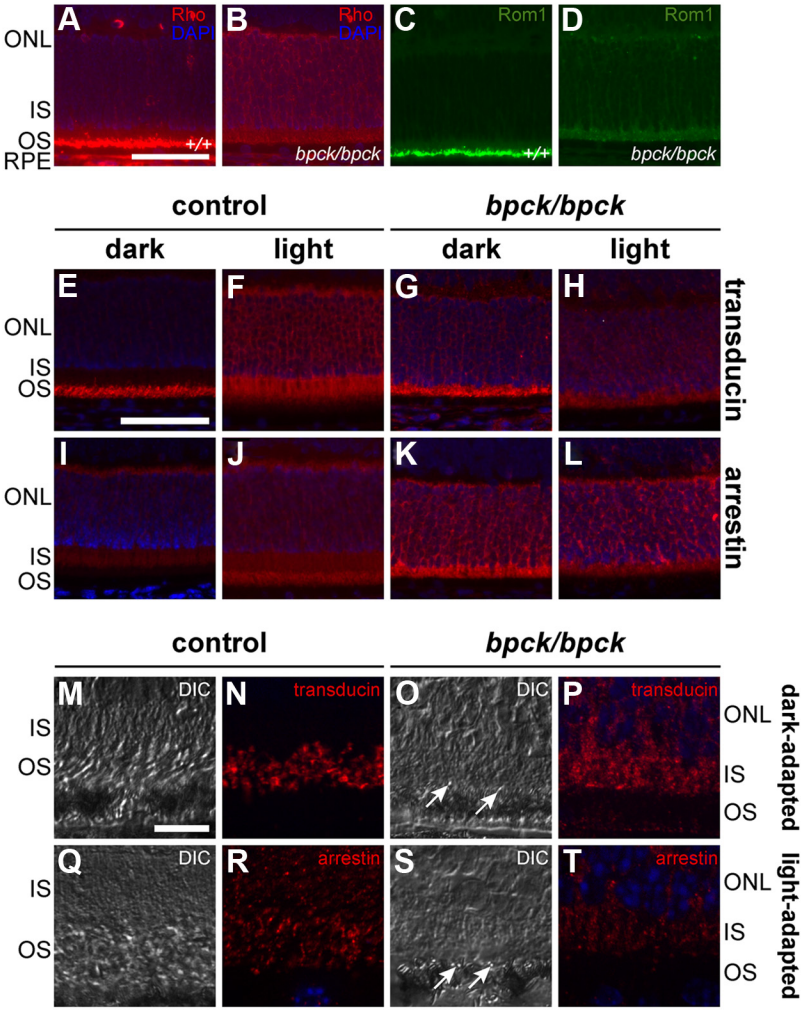

FIGURE 5. Transport of proteins is impaired in *bpck/bpck* mutants. (**A–D**) Mislocalization of actively transported OS proteins, rhodopsin and ROM1. P12 control and *bpck/bpck* mutant retinas were immunostained with (**A**, **B**) anti-rhodopsin and (**C**, **D**) anti-ROM1. In control retinas, rhodopsin and ROM1 localize to the photoreceptor OS. In contrast, in P12 *bpck/bpck* mutant retinas, both rhodopsin and ROM1 mislocalize to the IS and ONL cell bodies and pedicules. (**E–L**) Light-induced translocation of transducin (**E–H**) and arrestin (**I–L**). In the dark-adapted state of P14 mutant retinas, transducin is abnormally distributed throughout the inner segments and ONL, whereas arrestin fails to translocate to the outer segments on light induction. (**M–T**) Differential interference contrast (DIC; **M**, **O**, **Q**, **S**) and high-resolution fluorescent (**N**, **P**, **R**, **T**) images of mutant and control IS–OSs. In the mutant retinas, there is no evidence of arrestin or transducin staining in the light- and dark-adapted residual OSs (*white arrows*), respectively. Scale bars: (**A–L**) 50 μm; (**M–T**) 10 μm.

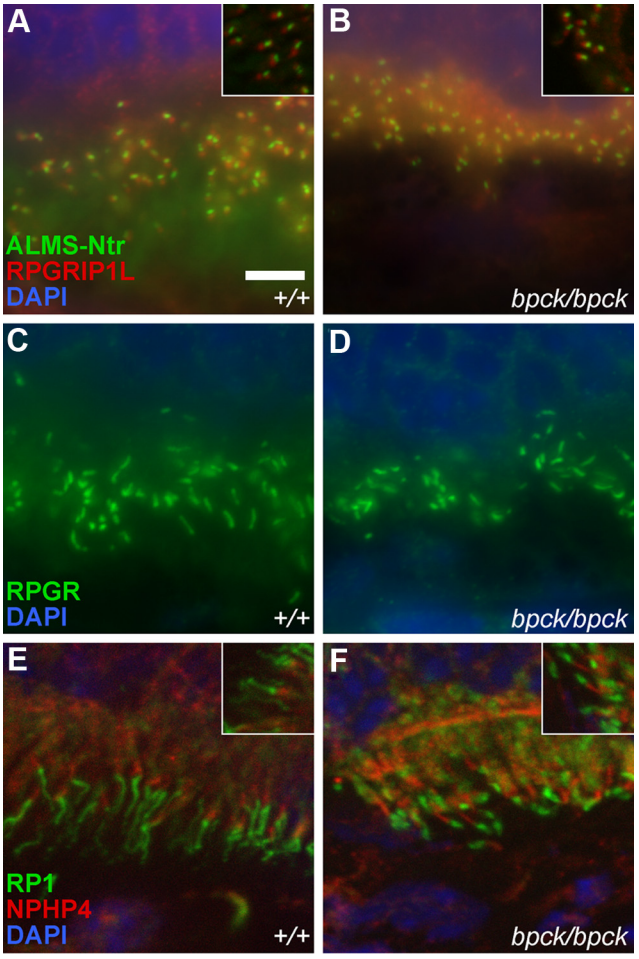

Figure 6. (**A**–**D**) Immunolocalization of photoreceptor ciliary proteins. At P12, both control (**A**, **C**) and mutant (**B**, **D**) retinas show normal staining with RPGRIP1L (*red*), ALMS1 (ALMS-Ntr; *green*), and RPGR (*green*), respectively. (**E**, **F**) At P14, immunostainings with RP1 (*green*) and NPHP4 (*red*) show a reduced length of the axonemal ciliary tip in mutants. Scale bars: 5 μm.

in P12 *bpck/bpck* mutant photoreceptors (Figs. 6A–D). In addition, costaining with NPHP4 (a ciliary transition zone protein that interacts with meckelin[34,35]) and RP1 (marker for the proximal ciliary axoneme[36]) showed normal localization at P14. However, the length of the RP1-stained ciliary tip was significantly shortened in mutant photoreceptors (Figs. 6E, 6F). These stunted axonemal ends are most likely the consequence of incomplete OS formation.

Tmem67^{bpck} Mutation Also Affects Cone Photoreceptors

Peanut agglutinin lectin (PNA) staining of photoreceptor cone sheaths at P12 revealed a similar number of cones in mutant and controls (Figs. 7A, 7B). However, the lengths of the cone sheaths were significantly reduced in mutants. Double staining with PNA-lectin and green opsin in retinal flat mounts of mutants revealed an aberrant localization of green opsin compared with controls (Figs. 7C, 7D). Further staining of green opsin in retinal sections revealed a mislocalization of the protein to the ONL (not shown). Similarly, blue opsin was mislocalized to the ONL in mutants (Figs. 7E, 7F). Toward the far dorsal regions of the retina, which are known to have fewer S cones,[37] a reduced number of blue opsin–stained photoreceptor cones were observed (not shown).

Discussion

Meckelin is a transmembrane and ciliary protein implicated in disorders such as Meckel–Gruber Syndrome (MKS), COACH Syndrome, Joubert Syndrome, Bardet–Biedl Syndrome, and Nephronophthisis that share common overlapping phenotypic features such as polycystic kidney disease, CNS abnormalities, and hepatic dysfunction. The role of MKS3 in retinal development and function has not been fully appreciated due to the embryonic lethal and/or perinatal lethal nature of MKS3 null mutations. However, eye abnormalities have been reported in a subset of patients with mutations in *MKS3* that include retinal coloboma, retinal degeneration, and oculomotor apraxia[38] and in the *wpk* rat model.[31]

In this report, we describe the retinal phenotype observed in homozygous *Tmem67*^{bpck} mutants. Due to the severity of hydrocephalus and/or rapid progression of PKD, mutants rarely survive into adulthood. However, in those mutants that do survive, panretinal dysmorphic patches of depigmented RPE and attenuation of blood vessels are observed at P34,

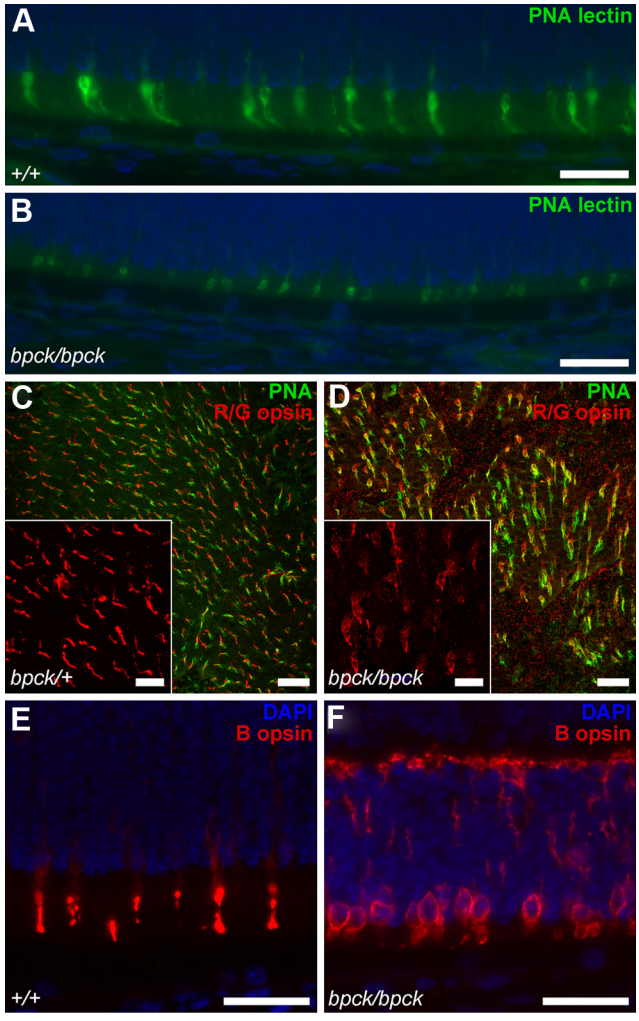

Figure 7. Cone opsin staining. PNA-lectin staining of (**A**) wild-type (+/+) and (**B**) *bpck/bpck* retinas reveals shortened photoreceptor cone sheaths in mutants compared with controls. Double staining PNA-lectin with *red-green* (R/G) opsin in controls and mutant flat-mount retinas show atypical staining of M cones. Immunostaining with *blue* (**B**) opsin in the ventral retina shows mislocalization of the protein to the ONL in P15 mutant retinas (**E**, **F**). Scale bars: (**A**–**D**) 20 μm; (**C**, **D**, *inset*) 10 μm; (**E**, **F**) 25 μm.

indicating early retinal defects in mice lacking a functional MKS3.

The Wistar *wpk* rat, originally described as a model for PKD, harbors a hypomorphic mutation, P394L, in the *Mks3/Tmem67* gene.[1] In addition to renal cysts, *wpk* rats exhibit CNS malformations and retinal and testicular defects. Histologic and ultrastructural studies in *wpk* rat retinas revealed significant photoreceptor degeneration at 3 weeks of age, the only time point reported.[31] Also, at 3 weeks, although photoreceptor cilia appeared structurally normal, OSs were not observed. This led the investigators to conclude that OSs did not form in *wpk* rats.[31]

Similar to the *wpk* rat model of MKS3, photoreceptor degeneration in *bpck* mice occurs early and progresses rapidly. However, our ultrastructural analysis of P8 and P12 retinas clearly show that although *bpck/bpck* mutants failed to develop normal OSs, rudimentary OSs were visible. At P14, the few membranous OS discs that were found in *bpck/bpck* mouse retinas were misshapen and disorganized. Therefore, MKS3 is not necessary for the initiation of OS development but instead for the elongation and maintenance of the OSs.

Although the architecture of the CC was typical with a "9+0" microtubular arrangement, indicating normal cilia assembly, the OS proteins rhodopsin and ROM1 did not properly localize to the outer segments and were found in the cell bodies of the ONL. Normally, rhodopsin is synthesized by ribosomes attached to the endoplasmic reticulum in photoreceptor ISs and travels to the Golgi, and then to the periciliary membrance complex where IFT cargo is assembled and transports rhodopsin through the CC to the outer segments.[39] The mislocalization of rhodopsin to the ONL is likely to be due in part to the lack of OS. However, meckelin must also be involved in the process of rhodopsin transport because no rhodopsin appears in the rudimentary OS. This is in contrast to other models such as $Pfdn5^{nmf5a28}$ and $Nphp4^{nmf19217}$ that have abnormal OSs, but still traffic rhodopsin to their OSs. The inner segments of $Tmem67^{bpck}$ retinas do not have an accumulation of vesicles that are commonly observed at the IS base in some retinal degenerative mutants.[40,41] Furthermore, the lack of vacuolar inclusions in the IS suggests the defect mediated by meckelin deficits occurs early in protein trafficking across the CC, perhaps in the internalization of rhodopsin into vesicles or in the trafficking of vesicles to the ciliary base.

Recent studies have revealed molecular interactions of MKS3 with MKS1,[16] SYNE2 (Nesprin2),[42] NPHP4,[34,35] TMEM216,[8] and TCTN1.[14] These proteins are likely to have roles in ciliary assembly and trafficking, centrosome migration, and cell-cycle regulation of centrosome duplication.[8,16,31,34] During in vitro ciliogenesis, disruption of meckelin and MKS1 results in the aberrant apical targeting and anchoring of the mother centriole to the plasma membrane (PM).[16] In our animal model in which meckelin is absent, the mother centriole was properly targeted to the apical membrane of the photoreceptor, suggesting that there must be other molecules that are able to compensate for the loss of meckelin function.

In conclusion, the *bpck/bpck* mouse model recapitulates many of the clinical features commonly seen in patients with disruptions in *MKS3*, including PKD, hydrocephaly, and retinal degeneration. The results shown here suggest meckelin may play a role in photoreceptor intraciliary transport and outer segment morphogenesis. Understanding the basis of ciliary dysfunction in the MKS3 retina may provide insights into the pathogenesis of other tissues in which it is expressed and allow for a better elucidation of the pathways and networks important in ciliary function.

Acknowledgments

The authors thank Muriel Davisson for providing the B6C3Fe *a/a-bpck/J* mice, JAX multimedia services for graphical assistance, and Pete Finger and Lesley Bechtold for EM imaging services.

References

1. Smith UM, Consugar M, Tee LJ, et al. The transmembrane protein meckelin (MKS3) is mutated in Meckel–Gruber syndrome and the wpk rat. *Nat Genet.* 2006;38:191–196.
2. Leitch CC, Zaghloul NA, Davis EE, et al. Hypomorphic mutations in syndromic encephalocele genes are associated with Bardet–Biedl syndrome. *Nat Genet.* 2008;40:443–448.
3. Brancati F, Travaglini L, Zablocka D, et al. RPGRIP1L mutations are mainly associated with the cerebello-renal phenotype of Joubert syndrome-related disorders. *Clin Genet.* 2008;74:164–170.
4. Doherty D, Parisi MA, Finn LS, et al. Mutations in 3 genes (MKS3, CC2D2A and RPGRIP1L) cause COACH syndrome (Joubert syndrome with congenital hepatic fibrosis). *J Med Genet.* 2010;47:8–21.
5. Baala L, Romano S, Khaddour R, et al. The Meckel–Gruber syndrome gene, MKS3, is mutated in Joubert syndrome. *Am J Hum Genet.* 2007;80:186–194.
6. Otto EA, Tory K, Attanasio M, et al. Hypomorphic mutations in meckelin (MKS3/TMEM67) cause nephronophthisis with liver fibrosis (NPHP11). *J Med Genet.* 2009;46:663–670.
7. Meckel JF. Beschreibung zweier, durch sehr ähnliche bidungsabweichungen entstelter geschwister. *Dtsch Arch Physiol.* 1822;7:99–172.
8. Valente EM, Logan CV, Mougou-Zerelli S, et al. Mutations in TMEM216 perturb ciliogenesis and cause Joubert, Meckel and related syndromes. *Nat Genet.* 2010;42:619–625.
9. Delous M, Baala L, Salomon R, et al. The ciliary gene RPGRIP1L is mutated in cerebello-oculo-renal syndrome (Joubert syndrome type B) and Meckel syndrome. *Nat Genet.* 2007;39:875–881.
10. Frank V, den Hollander AI, Bruchle NO, et al. Mutations of the CEP290 gene encoding a centrosomal protein cause Meckel–Gruber syndrome. *Hum Mutat.* 2008;29:45–52.
11. Tallila J, Jakkula E, Peltonen L, Salonen R, Kestila M. Identification of CC2D2A as a Meckel syndrome gene adds an important piece to the ciliopathy puzzle. *Am J Hum Genet.* 2008;82:1361–1367.
12. Hopp K, Heyer CM, Hommerding CJ, et al. B9D1 is revealed as a novel Meckel syndrome (MKS) gene by targeted exon-enriched next-generation sequencing and deletion analysis. *Hum Mol Genet.* 2011;20:2524–2534.
13. Shaheen R, Faqeih E, Seidahmed MZ, et al. A TCTN2 mutation defines a novel Meckel Gruber syndrome locus. *Hum Mutat.* 2011;32:573–578.
14. Garcia-Gonzalo FR, Corbit KC, Sirerol-Piquer MS, et al. A transition zone complex regulates mammalian ciliogenesis and ciliary membrane composition. *Nat Genet.* 2011;43:776–784.
15. Coene KL, Mans DA, Boldt K, et al. The ciliopathy-associated protein homologs RPGRIP1 and RPGRIP1L are linked to cilium integrity through interaction with Nek4 serine/threonine kinase. *Hum Mol Genet.* 2011;20:3592–3605.
16. Dawe HR, Smith UM, Cullinane AR, et al. The Meckel–Gruber Syndrome proteins MKS1 and meckelin interact and are required for primary cilium formation. *Hum Mol Genet.* 2007;16:173–186.
17. Won J, Marin de Evsikova C, Smith RS, et al. NPHP4 is necessary for normal photoreceptor ribbon synapse maintenance and outer segment formation, and for sperm development. *Hum Mol Genet.* 2011;20:482–496.
18. Liu Q, Lyubarsky A, Skalet JH, Pugh EN Jr, Pierce EA. RP1 is required for the correct stacking of outer segment discs. *Invest Ophthalmol Vis Sci.* 2003;44:4171–4183.
19. Zhao Y, Hong DH, Pawlyk B, et al. The retinitis pigmentosa GTPase regulator (RPGR)- interacting protein: subserving RPGR function and participating in disk morphogenesis. *Proc Natl Acad Sci USA.* 2003;100:3965–3970.
20. Won J, Gifford E, Smith RS, et al. RPGRIP1 is essential for normal rod photoreceptor outer segment elaboration and morphogenesis. *Hum Mol Genet.* 2009;18:4329–4339.

21. Chang B, Khanna H, Hawes N, et al. In-frame deletion in a novel centrosomal/ciliary protein CEP290/NPHP6 perturbs its interaction with RPGR and results in early-onset retinal degeneration in the rd16 mouse. *Hum Mol Genet.* 2006;15:1847–1857.
22. Swiderski RE, Nishimura DY, Mullins RF, et al. Gene expression analysis of photoreceptor cell loss in bbs4-knockout mice reveals an early stress gene response and photoreceptor cell damage. *Invest Ophthalmol Vis Sci.* 2007;48:3329–3340.
23. Westfall JE, Hoyt C, Liu Q, et al. Retinal degeneration and failure of photoreceptor outer segment formation in mice with targeted deletion of the Joubert syndrome gene, Ahi1. *J Neurosci.* 2010;30: 8759–8768.
24. Pazour GJ, Baker SA, Deane JA, et al. The intraflagellar transport protein, IFT88, is essential for vertebrate photoreceptor assembly and maintenance. *J Cell Biol.* 2002;157:103–113.
25. Insinna C, Besharse JC. Intraflagellar transport and the sensory outer segment of vertebrate photoreceptors. *Dev Dyn.* 2008;237: 1982–1992.
26. LaVail MM. Kinetics of rod outer segment renewal in the developing mouse retina. *J Cell Biol.* 1973;58:650–661.
27. Young RW. The renewal of photoreceptor cell outer segments. *J Cell Biol.* 1967;33:61–72.
28. Lee Y, Smith RS, Jordan W, et al. Prefoldin 5 is required for normal sensory and neuronal development in a murine model. *J Biol Chem.* 2011;286:726–736.
29. Cook SA, Collin GB, Bronson RT, et al. A mouse model for Meckel syndrome type 3. *J Am Soc Nephrol.* 2009;20:753–764.
30. Strauss WM. Preparation of genomic DNA from mammalian tissue. *Curr Protoc Mol Biol.* 1998;(suppl 42):2.2.1–2.2.3.
31. Tammachote R, Hommerding CJ, Sinders RM, et al. Ciliary and centrosomal defects associated with mutation and depletion of the Meckel syndrome genes MKS1 and MKS3. *Hum Mol Genet.* 2009; 18:3311–3323.
32. Hearn T, Spalluto C, Phillips VJ, et al. Subcellular localization of ALMS1 supports involvement of centrosome and basal body dysfunction in the pathogenesis of obesity, insulin resistance, and type 2 diabetes. *Diabetes.* 2005;54:1581–1587.
33. Hong DH, Pawlyk B, Sokolov M, et al. RPGR isoforms in photoreceptor connecting cilia and the transitional zone of motile cilia. *Invest Ophthalmol Vis Sci.* 2003;44:2413–2421.
34. Williams CL, Masyukova SV, Yoder BK. Normal ciliogenesis requires synergy between the cystic kidney disease genes MKS-3 and NPHP-4. *J Am Soc Nephrol.* 2010;21:782–793.
35. Williams CL, Li C, Kida K, et al. MKS and NPHP modules cooperate to establish basal body/transition zone membrane associations and ciliary gate function during ciliogenesis. *J Cell Biol.* 2011;192: 1023–1041.
36. Liu Q, Zhou J, Daiger SP, et al. Identification and subcellular localization of the RP1 protein in human and mouse photoreceptors. *Invest Ophthalmol Vis Sci.* 2002;43:22–32.
37. Applebury ML, Antoch MP, Baxter LC, et al. The murine cone photoreceptor: a single cone type expresses both S and M opsins with retinal spatial patterning. *Neuron.* 2000;27:513–523.
38. Gunay-Aygun M, Parisi MA, Doherty D, et al. MKS3-related ciliopathy with features of autosomal recessive polycystic kidney disease, nephronophthisis, and Joubert Syndrome. *J Pediatr.* 2009;155: 386–392.
39. Deretic D, Schmerl S, Hargrave PA, Arendt A, McDowell JH. Regulation of sorting and post-Golgi trafficking of rhodopsin by its C-terminal sequence QVS(A)PA. *Proc Natl Acad Sci USA.* 1998;95: 10620–10625.
40. Hagstrom SA, Duyao M, North MA, Li T. Retinal degeneration in tulp1−/− mice: vesicular accumulation in the interphotoreceptor matrix. *Invest Ophthalmol Vis Sci.* 1999;40:2795–2802.
41. Collin GB, Cyr E, Bronson R, et al. Alms1-disrupted mice recapitulate human Alstrom syndrome. *Hum Mol Genet.* 2005;14:2323–2333.
42. Dawe HR, Adams M, Wheway G, et al. Nesprin-2 interacts with meckelin and mediates ciliogenesis via remodelling of the actin cytoskeleton. *J Cell Sci.* 2009;122:2716–2726.